

Short Note

On the Proper Setup of the Double Mach Reflection as a Test Case for the Resolution of Gas Dynamics Codes

Friedemann Kemm*

May 5, 2014

Keywords: Double Mach reflection, high speed flow, high resolution scheme, numerical test case

MSC 2010: 76J20, 76L05, 76M99

This note discusses the initial and boundary conditions as well as the size of the computational domain for the double Mach reflection problem when set up as a test for the resolution of an Euler scheme for gas dynamics.

1 The double Mach reflection

A famous test for the quality of a Riemann solver is the Double Mach reflection problem. It was suggested by Woodward and Colella [11] as a benchmark for Euler codes. An analytical treatment is found in [9] and [1] and the references therein, while experimental results are presented in [3] and also in [1, pp. 152 and 168]. The problem consists of a shock front that hits a ramp which is inclined by 30 degrees. When the shock runs up the ramp, a self similar shock structure with two triple points evolves. The situation is sketched out in Figure 1. To simplify the graphical representation, the coordinate system is aligned with the ramp – as done for the numerical tests. In the primary triple point, the incident shock i , the mach stem m , and the reflected shock r meet. In the double mach configuration, the

*Brandenburg University of Technology, Platz der Deutschen Einheit 1, 03046 Cottbus, Germany, kemm@math.tu-cottbus.de

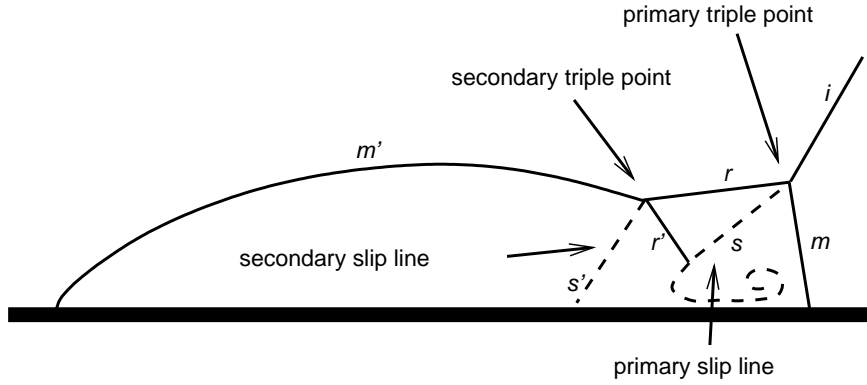


Figure 1: Sketch of the double Mach reflection problem. The bottom line represents the ramp.

reflected shock breaks up forming a secondary triple point with the reflected shock r , a secondary (bowed) mach stem m' , and a secondary reflected shock r' . From both triple points, slip lines emanate. The reflected shock r' hits the primary slip line s causing a curled flow structure, the resolution of which may serve as an indicator for the resolution of a numerical scheme. But—as was already stated by Woodward and Colella—the main challenge for a high resolution scheme is to resolve the secondary slip line s' . Being a rather weak feature, it is hardly visible in a density plot or a plot of any velocity component. According to Woodward and Colella [11], the secondary slip s' line can be best observed in the vertical momentum. Thus, throughout this paper we present the results for the vertical momentum ρv .

2 The problem: two issues

For our numerical tests, we use the setting as described in [11]. We start with the shock already on the ramp and rotate the coordinate system and, so that the computational grid is aligned with the ramp. The initial conditions left and right of the shock are

$$\begin{aligned} \rho_l &= 8.0, & (\rho u)_l &= 57.1597, & (\rho v)_l &= -33.0012, & E_l &= 563.544, \\ \rho_r &= 1.4, & (\rho u)_r &= 0, & (\rho v)_r &= 0, & E_r &= 2.5. \end{aligned}$$

The initial shock hits the bottom of the computational domain at $x_0 = 1/6$. Usually the computational domain is chosen as $[0, 4] \times [0, 1]$ and the results are presented for $t = 0.2$. At the bottom, we employ solid wall conditions, at the right boundary outflow. At all other boundaries we use Dirichlet-conditions, which are set to the physical values.

Unfortunately, as the results in Figure 2 show, there are severe disturbances of the flow close to the secondary slip line. Depending on the scheme and the grid resolution, it is difficult to distinguish between slip line and numerical artifact.

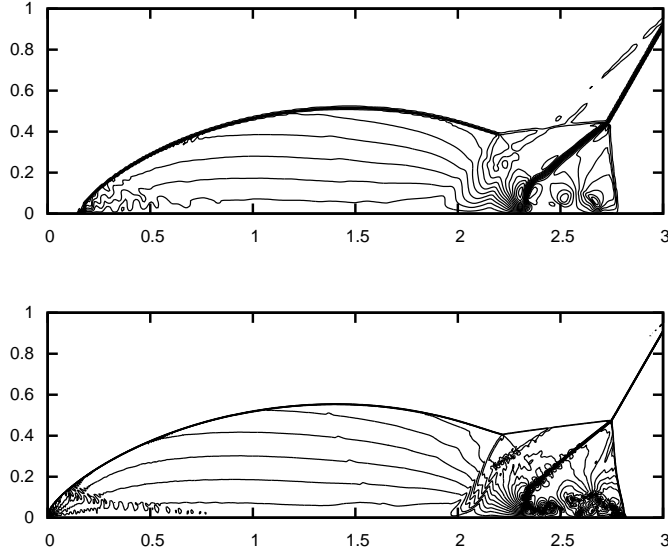


Figure 2: Numerical artifact near the secondary slip line in the standard setting with $\Delta x = \Delta y = 1/120$ (top) and $\Delta x = \Delta y = 1/480$ (bottom).

As Figure 2 shows, this setting results in some numerical artifacts disturbing the secondary reflected shock r' and the region between the secondary reflected shock and the secondary slip line. At lower resolutions (top picture), the artifacts are not distinguishable from the secondary slip line s' . While Woodward and Colella [11] blame this effect to the under-resolved shock in the initial condition, Rider et al. [10] argue that the under-resolved shock in the boundary condition for the upper boundary is responsible for it. Both are partially right and partially wrong: In Figure 3, we show results for the double Mach reflection computed on $[0, 4] \times [0, 2]$ instead of $[0, 4] \times [0, 1]$. It can be seen that what in Figure 2 seemed to be one (kinked) phenomenon in fact are two artifacts: one arising from the shock position at the upper boundary—it shows up as a slight disturbance above the shock close to the right boundary and as a slight disturbance a little bit left of the secondary slip line—and one that follows the shock at a certain distance (and slightly to the right of the secondary slip line), indicating that it results from the initial condition. This means that there indeed is an artifact arising from the initial condition (hypothesis by Woodward and Colella) and an artifact arising from the boundary condition (hypothesis by Rider et al.).

In the following, we will investigate both hypotheses by means of numerical tests with different settings. This will give us some hints on the proper use of the double Mach reflection as a test case for Euler codes.

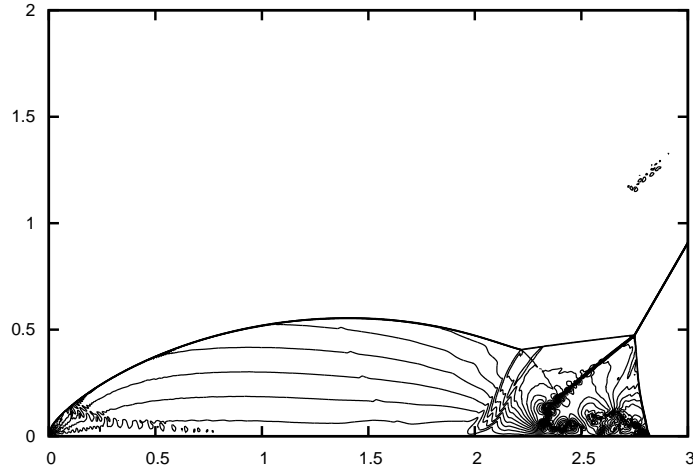


Figure 3: Double Mach reflection computed on $[0, 4] \times [0, 2]$.

3 The numerical environment for the tests

To set up tests in order to investigate the hypotheses by Rider et al. and by Woodward and Colella, one has to make sure that the grid resolution is the only variable parameter in the numerical scheme. Besides this, the size of the computational domain and the initial and the boundary conditions may vary. But the basic features of the method have to be fixed, including Riemann solver, grid structure, basic approach (finite differences, finite volumes, discontinuous Galerkin, ...), reconstruction techniques, limiters, time scheme etc. In this study, we resort to finite volumes on a uniform equidistant Cartesian grid with $\Delta x = \Delta y$. The basic scheme uses wave propagation according to LeVeque [8] with algebraic limiting and Roe with Harten-Hyman entropy fix [4]. Thus, it is a second order TVD-scheme. The second order corrections are applied also for the corner fluxes. As limiter, we employ the mixed use of CFL-Superbee and Superpower as described in [6], modified for nonlinear waves according to Jeng and Payne [5] as described in [7]. The code used for the examples is clawpack [2]. As for Figure 2, we do not show the entire computational domain. We restrict the x -direction to $[0, 3]$ or, in Figure 4, show a close-up of the region of interest: the region containing the triple points. As already mentioned, the quantity shown is always the vertical momentum ρv . And, if not stated otherwise, the grid resolution is $\Delta x = \Delta y = 1/480$.

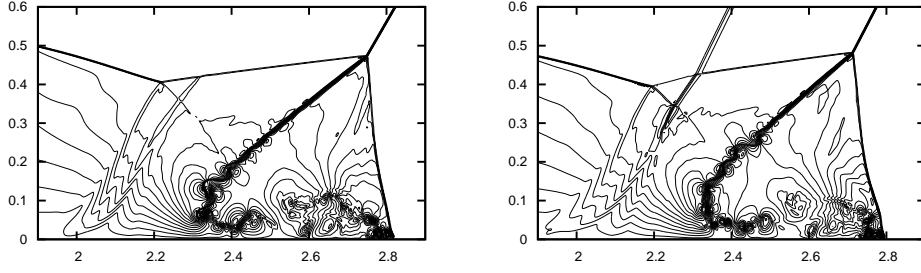


Figure 4: Effect of boundary condition at top boundary: Dirichlet (left) and oblique extrapolation (right).

4 Hypothesis by Rider et al.

According to Rider et al. [10], the under-resolved shock in the boundary condition forces a reflection phenomenon which can be avoided if the shock is smeared over three grid cells. The tests in Figure 2 were executed with such a setting. Obviously, for high grid resolutions, this is not sufficient. Even smearing over seven grid cells would not give the desired results. Furthermore, it is not at all clear if a linear smearing would be appropriate or if a more complex strategy has to be chosen.

Another idea would be to switch the boundary conditions at the upper boundary from Dirichlet to oblique first-order extrapolation. Since the angle of the shock to the vertical grid lines is 30° , for $\Delta x = \Delta y$ this can be easily achieved by setting

$$q_{i,m+1} = q_{i-1,m-1}, \quad q_{i,m+2} = q_{i-1,m}, \quad (1)$$

where m is the number of grid cells in the y -direction. As Figure 4 indicates, the reflection is no longer seen. However, the shock runs, also the angle of the primary shock changes over time and, thus, changes the structure of the solution. It is no longer self-similar. Furthermore, the extrapolation enhances the resolution of the other numerical artifact and, thus, deteriorates the quality of the solution even more.

In summary, the best strategy to address the reflection from the top boundary is—as shown for Figure 3 in the previous section—to enlarge the computational domain in the y -direction. This way, one can make sure that it preserves the self-similar structure of the solution and, at the same time, does not interact with the secondary slip line. It hits the secondary Mach stem m' far left of the interesting part of the solution.

5 Hypothesis by Woodward and Colella

While the artifact arising from the boundary condition can easily be removed from the region of interest, this is not true for the artifact arising from the initial condition which is part

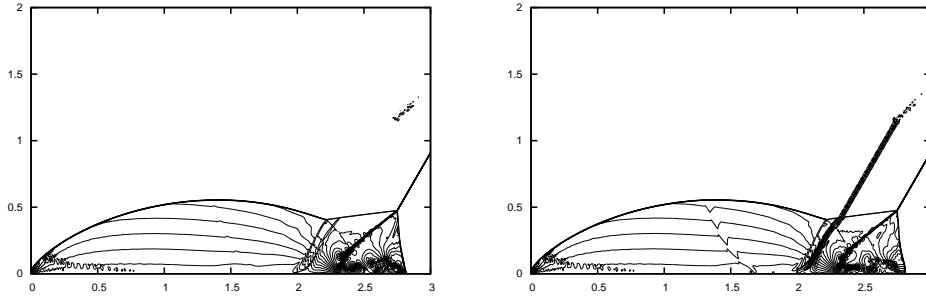


Figure 5: Effect of initial condition: with sharp initial shock (left), with smeared initial shock (right).

of the self-similar numerical—not of the physical—structure of the solution. According to Woodward and Colella [11], the artifact arising from the initial condition results from the fact that a shock which does not start at a grid line, but is somehow projected onto the grid, is automatically under-resolved.

Therefore, smearing the shock in the initial condition should show some considerable improvement. However, Figure 5 reveals quite the opposite. Essentially, there is no general way to represent a non-grid-aligned shock without forcing unphysical waves arising from the initial oblique Riemann problem. It seems even doubtful whether this might work for any shock capturing scheme, no matter how much information on the scheme is invested in the construction of the discrete initial state.

6 Consequences for the setup of the double Mach reflection as a test

Although the presented results are gained on a fixed uniform grid, we can draw some conclusions for both cases: (1) Test with fixed grid resolution, which is intended to test the quality of the basic scheme; (2) Test with an adaptive grid, which mainly tests the quality of the refinement/coarsening strategy.

(1) With fixed grid resolution: The artifact due to the under-resolved shock in the boundary condition for the upper boundary can be easily removed from the region of interest by enlarging the computational domain in the y -direction. For $[0, 4] \times [0, 2]$ instead of $[0, 4] \times [0, 1]$, the artifact is far left of the secondary triple point and the secondary slip line. We have found that it is essentially impossible to get rid of the artifact due to the under-resolved initial shock. In order to get information on the quality of the basic numerical scheme, we need to ensure that the grid is fine enough to separate the numerical artifact from the secondary slip line, cf. Figure 2.

(2) With adaptive grid resolution: To test the quality of a grid refinement/coarsening strategy, it is reasonable to keep the original setting of Woodward and Colella. A good refinement/coarsening strategy has to make sure that physical features like the secondary slip line are refined while numerical artifacts are not. They have to be invisible in the numerical results, while the secondary slip line has to be well resolved.

References

- [1] Gabi Ben-Dor. *Shock wave reflection phenomena. 2nd ed.* Shock Wave and High Pressure Phenomena. Berlin: Springer. xiii, 342 p., 2007.
- [2] Clawpack (conservation laws package). <http://www.amath.washington.edu/claw>.
- [3] LG Gvozdeva, OA Predvoditeleva, and VP Fokeev. Double mach reflection of strong shock waves. *Fluid Dynamics*, 3(1):6–11, 1968.
- [4] Amiram Harten and James M. Hyman. Self adjusting grid methods for one-dimensional hyperbolic conservation laws. *J. Comput. Phys.*, 50(2):235–269, 1983.
- [5] Yih Nen Jeng and Uon Jan Payne. An adaptive TVD limiter. *J. Comput. Phys.*, 118(2):229–241, 1995.
- [6] Friedemann Kemm. A comparative study of TVD limiters – well known limiters and an introduction of new ones. *Internat. J. Numer. Methods Fluids*, 67(4):404–440, 2011.
- [7] Friedemann Kemm. Cfl-number-dependent tvd-limiters. In Elena Vázquez-Cendón, Arturo Hidalgo, Pilar García-Navarro, and Luis Cea, editors, *Numerical Methods for Hyperbolic Equations: Theory and Applications*, pages 277–283. CRC Press, 2012. Proceedings of the international conference on Numerical Methods for Hyperbolic Equations: Theory and Applications, Santiago de Compostela, Spain, 4–9 July 2011.
- [8] Randall J. Leveque. *Finite volume methods for hyperbolic problems.* Cambridge Texts in Applied Mathematics. Cambridge: Cambridge University Press, 2002.
- [9] H. Li and G. Ben-Dor. A shock dynamics theory based analytical solution of double Mach reflections. *Shock Waves*, 5(4):259–264, 1995.
- [10] William J. Rider, Jeffrey A. Greenough, and James R. Kamm. Accurate monotonicity- and extrema-preserving methods through adaptive nonlinear hybridizations. *J. Comput. Phys.*, 225(2):1827–1848, 2007.
- [11] Paul Woodward and Phillip Colella. The numerical simulation of two-dimensional fluid flow with strong shocks. *J. Comput. Phys.*, 54:115–173, 1984.